Aust. J. Phys., 1995, **48**, 411–18

Silent Discharges in Ozonisers and CO_2 Lasers*

S. Yagi and M. Kuzumoto

Central Research Laboratory, Mitsubishi Electric Corporation,
Tsukaguchi-Honmachi 8-chome, Amagasaki, Hyogo, 661, Japan.

Abstract

Dielectric barrier ac discharges (silent discharges) have been developed to optimise the performance of ozonisers and CO_2 lasers. The characteristics and properties of the discharge are discussed and examined in the light of experimental results. The frequency of the applied voltage and gap length are around 1 kHz and 1 mm for the ozoniser and around 100 kHz and several cm for the CO_2 laser. We have found that ozone is produced with high efficiency by using high energy electrons in a narrow gap. On the other hand, for CO_2 lasers, a high excitation efficiency is achieved by specifying the laser medium gas at very high N_2 concentrations in a long gap.

1. Introduction

Silent discharges (SD or the dielectric barrier ac discharge), generated by applying an alternating high voltage between two electrodes covered with dielectrics, are widely used in ozone generators for chemical and industrial processes such as water treatment (Eliasson *et al.* 1987). In addition to ozonisers, SD excited CO_2 lasers for material processing such as metal cutting and welding have been developed (Yagi *et al.* 1977; Kuzumoto *et al.* 1987).

Comparative studies of present industrial applications of SD are necessary to develop other applications of silent discharges, for example, excimer lamps and plasma processing equipment. In this paper, the excitation characteristics and the properties of silent discharges are discussed and examined.

2. Silent Discharges in Ozonisers and CO_2 Lasers

Commercial ozonisers and CO_2 lasers and the configuration of their electrodes are shown in Figs 1 and 2. The discharge conditions for both cases are compared in Table 1.

The frequency of the applied voltage is usually below a few kHz and the gap length is around 1 mm for an ozoniser. On the other hand, these values are around 100 kHz and several cm for CO_2 lasers. We classify the former discharge as a low frequency SD and the latter as a high frequency SD. An example of a

* Refereed paper based on a presentation to the Third Japan–Australia Workshop on Gaseous Electronics and Its Applications, held at Yeppoon, Queensland, in July 1994.

0004-9506/95/030411$05.00

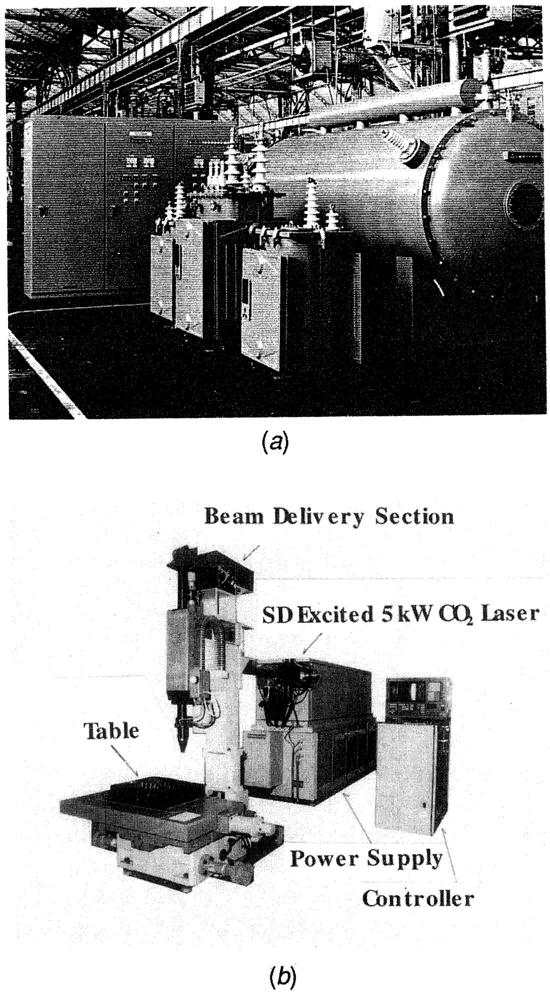

Fig. 1. Photographs of (*a*) the ozoniser (7·5 kg O_3 per hour) and (*b*) the CO_2 laser.

set of typical parameters in an ozoniser and a CO_2 laser used in industry is listed in Table 2.

(2a) Discharge Phenomena

Typical V–Q Lissajous figures observed at applied voltage frequencies of 2, 50 and 100 kHz are shown in Fig. 3. The horizontal and vertical axes show the applied voltage V and the electrical charge Q respectively. The Lissajous figure changes with the applied voltage frequency. At a frequency below 2 kHz, the figure shows a parallelogram. The figure changes into an ellipse with an increase in frequency.

We have proposed a new equivalent circuit for the high frequency silent discharge as shown in Fig. 4 (Tanaka *et al.* 1984), where C_g and C_0 are the

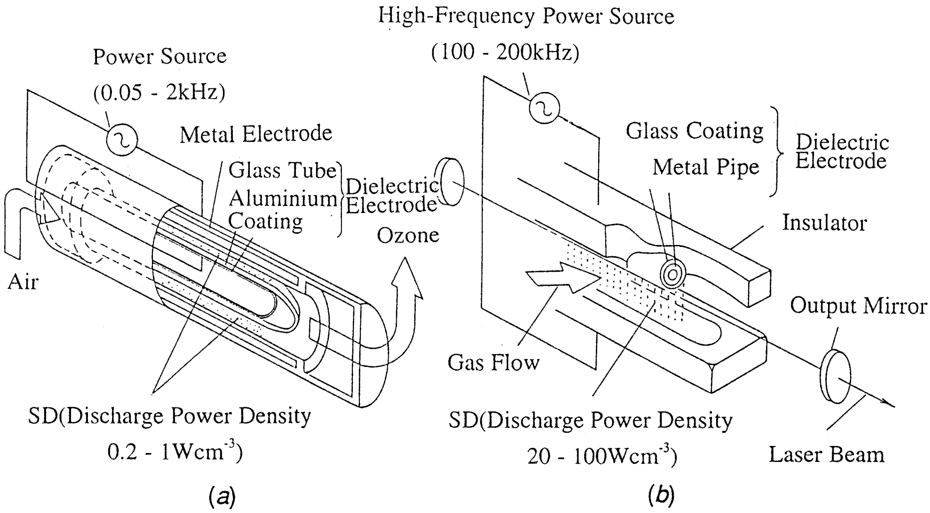

Fig. 2. Configuration of the electrodes for (*a*) the ozoniser and (*b*) the CO_2 laser.

Table 1. Conditions of discharge

Application	Frequency	Gap length	Pressure	Power density	Gas
Ozoniser	50 Hz–3 kHz	0·5–2 mm	760–2000 Torr	0·2–1 W cm^{-3}	Air, N_2, O_2
CO_2 Laser	50–200 kHz	20–50 mm	50–100 Torr	20–100 W cm^{-3}	CO_2–N_2–He

Table 2. Typical parameters in ozonisers and CO_2 lasers

	Ozoniser[A]	CO_2 laser[B]
Discharge	Low frequency SD distributed column	High frequency SD uniformly diffused
Gas species	Air	CO_2+CO+N_2+He
Pressure	1·7 atm	0·085 atm (65 Torr)
Gap spacing	1·2 mm	42 mm
E/N	1·1×10^{-15} V cm^2 (110 Td)	4·5×10^{-16} V cm^2 (45 Td)
Power density	0·2 W cm^{-2} (0·6 W cm^{-3})	57 W cm^{-2} (13·5 W cm^{-3})
Mechanism	Discharge chemistry	Discharge excitation → induced emission
Efficiency	(to produce O_3)	(to produce photon)
Theoretical limit	48%	42%
Practical	6%	10% (TEM_{00} mode)
Role of N_2	Energy pool to $N_2^*+O_2 \rightarrow O+O+N_2$	Energy pool to $N_2(V)+CO_2 \rightarrow CO_2(V)+N_2$
Gas cooling	Diffusion	Convection (v = 80 m s^{-1})
Gas temperature in discharge zone	310 K	350 K

[A] Mitsubishi ozoniser OS-25V. [B] Mitsubishi CO_2 laser, ML3016F3.

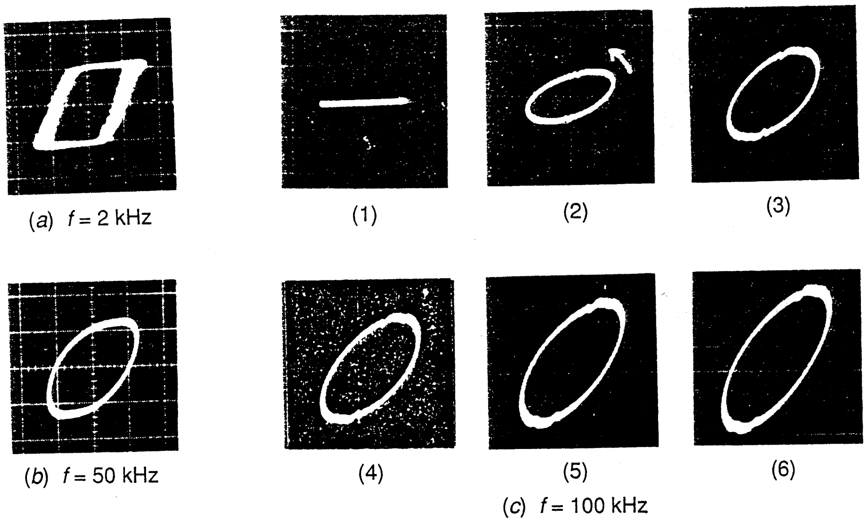

Fig. 3. The V–Q Lissajous figure where the horizontal voltage is 5 kV/div and the vertical charge is $6 \cdot 7$ μC/div and where $d = 4 \cdot 0$ cm and $P = 60$ Torr.

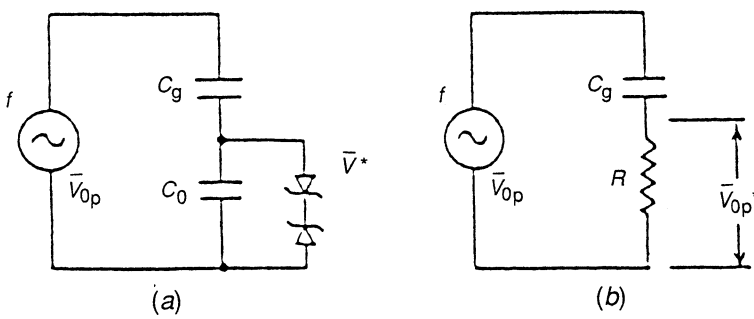

Fig. 4. Equivalent circuit for (a) conventional low frequency and (b) new high frequency.

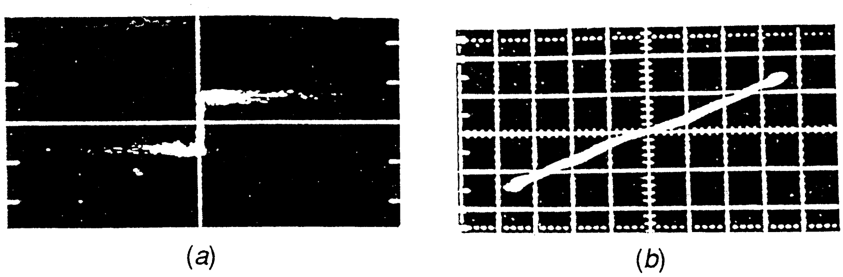

Fig. 5. The V_{gap}–current characteristics for (a) low frequency ($f = 2$ kHz) and (b) high frequency ($f = 100$ kHz), where the horizontal current is 1 A/div and the vertical voltage is 2 kV/div.

capacitances of the electrode and discharge gap, and R is the equivalent discharge resistance at a constant discharge voltage of V_{0p}^* (peak value) and f is the frequency. The model was deduced by considering the trapping of ions in the discharge gap. When a sinusoidal wave with the peak voltage V_{0p} is applied to the equivalent circuit shown in Fig. 4, the discharge power at low frequency SD is calculated from the model by (Tabata and Yagi 1975)

$$W = fC_g 2V^* \left\{ 2V_{0p} - \left(1 + \frac{C_0}{C_g}\right) 2V^* \right\} \approx 4fC_g V^*(V_{0p} - V^*) . \tag{1}$$

On the other hand, the discharge power at high frequency is given by (Tanaka *et al.* 1984)

$$W = \pi f C_g V_{0p}^* \sqrt{V_{0p}^2 - V_{0p}^{*2}} . \tag{2}$$

It has been found experimentally that V_{0p}^* is nearly equal to V^*.

The characteristics of the discharge voltage in the gap and the discharge current observed experimentally are shown in Fig. 5. The experimental figures agree well with the theoretical expectations from the model in Fig. 4.

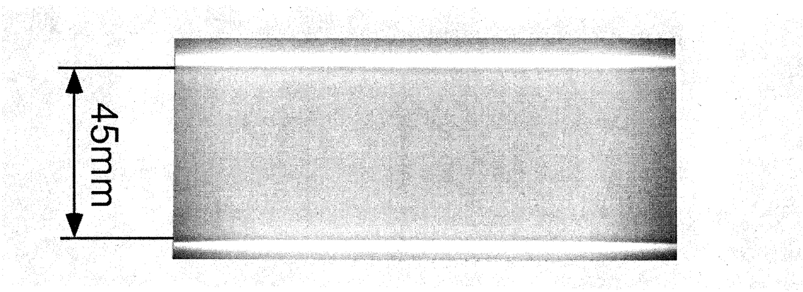

Fig. 6. A high-frequency silent discharge for $d = 45$ mm and $p = 50$ Torr in CO_2 laser gas.

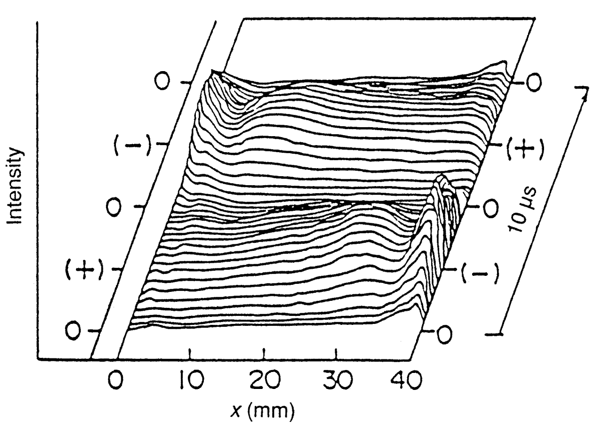

Fig. 7. Time resolved measurements of discharge emission for $d = 40$ mm and $p = 50$ Torr in a CO_2 laser gas.

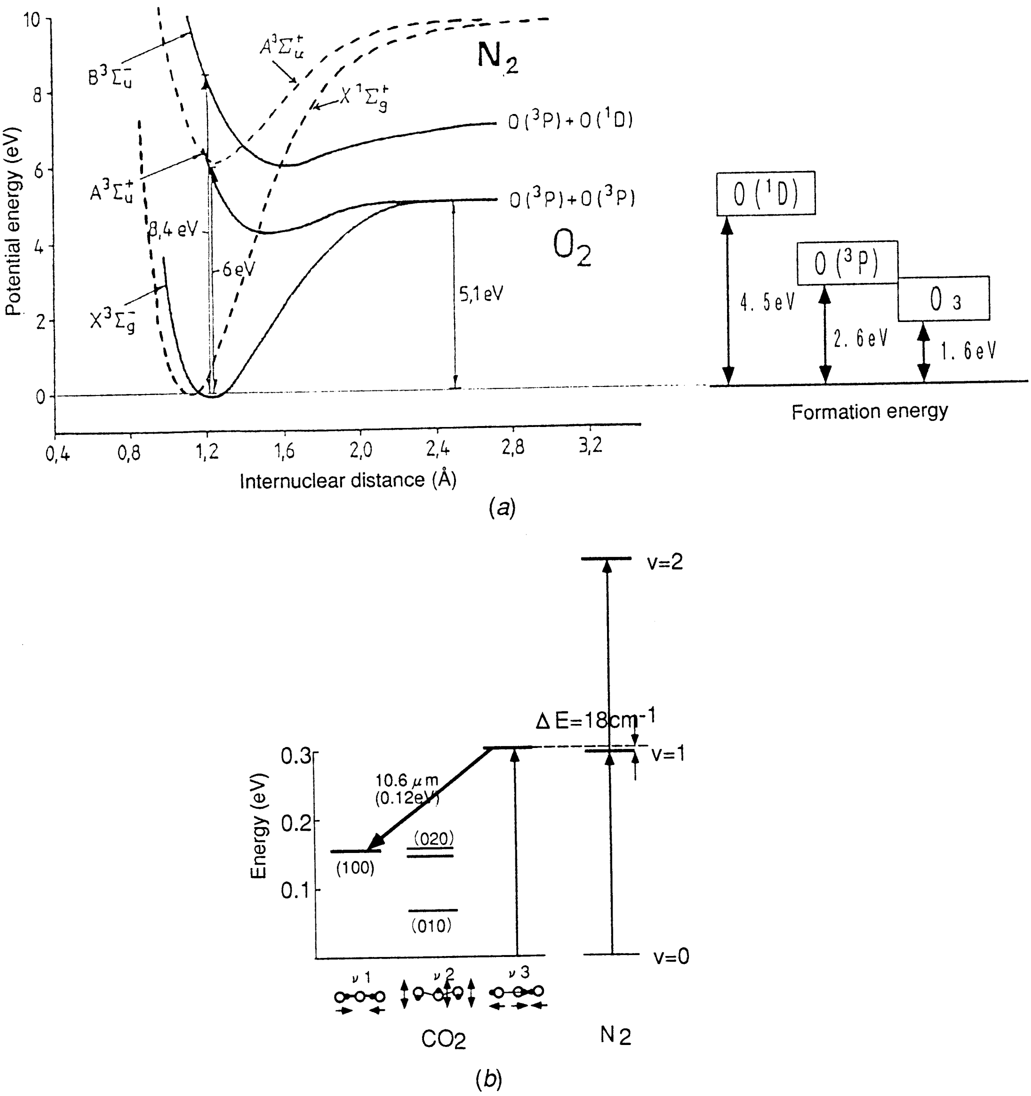

Fig. 8. Energy diagram for (*a*) the ozoniser and (*b*) the CO_2 laser.

A silent discharge consists of many time-varying micro-discharges. The charge created by one micro-discharge is of the order of 10^{-9} to 10^{-10} C and the main luminous time is less than 10 ns. A photograph of a high-frequency silent discharge for a CO_2 laser is shown in Fig. 6. The gap length is 45 mm, the gas composition is CO_2–CO–N_2–He = 8–4–60–28% and the gas pressure is 50 Torr (1 Torr ≡ 133 Pa). The discharge is very diffuse, uniform and stable. Time resolved measurements of the discharge emission are given in Fig. 7 (Kuzumoto and Yagi 1990). The emission lines are basically those of the second positive group of N_2 molecules. The same discharge is observed to take place in every half cycle of the applied voltage. A more luminous region is observed near the dielectric surface of the negative electrode. On the other hand, a brighter luminous region is observed near the positive electrode in the case of air.

(2b) Production Mechanism

Energy diagrams for the ozonisers and CO_2 laser are shown in Fig. 8. The minimum potential energy for initial excitation in ozonisers lie at 8·4 or 6 eV, while that for the CO_2 laser is around 0·3 eV or integral multiples of 0·3 eV. Relatively high energy electrons are required for ozonisers, while low energy electrons are required for CO_2 lasers.

The maximum efficiencies of commercial ozone generators are between about 5% to 20%. Lower values characterise air-fed ozonisers. The performances of oxygen-fed ozonisers are approximately only two times better; nevertheless, the oxygen concentration in air is five times less than that in pure oxygen gas. This phenomenon can be explained by the influence of metastable excited nitrogen molecules, which produce oxygen atoms by a collision with O_2 as shown in the following reactions, where N_2 molecules act as an energy pool for the initial step in ozone formation (Tabata *et al.* 1978; Eliasson *et al.* 1985):

$$\begin{aligned} &e + N_2(X'\Sigma_g^+) \rightarrow N_2(A^3\Sigma_u^+) + e\,, \\ &N_2(A^3\Sigma_u^+) + O_2 \rightarrow N_2(X'\Sigma_g^+) + 2O(^3P)\,, \\ &O(^3P) + O_2(X^3\Sigma_g^{-+}) + M \rightarrow O_3(^{12}A) + M\,. \end{aligned} \tag{3}$$

High efficiencies are realised by operating with a thin gap around 1 mm and a high pressure around 2 atm (1 atm ≡ 101·3 kPa). A thin gap keeps electron energies high and improves gas cooling effects. High pressure operation leads to a high probability of three body collisions between oxygen and neutral particles.

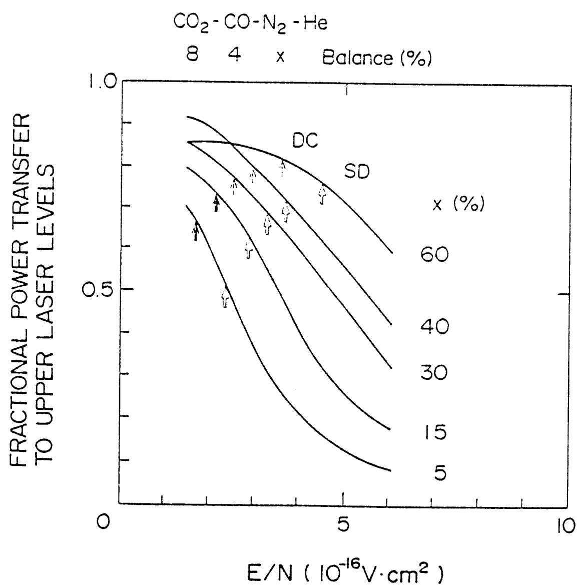

(↑), ⇧: Effective E/N for DC and SD excitation

Fig. 9. Excitation efficiency characteristics for a CO_2 laser.

Excitation efficiencies of the SD-CO_2 laser calculated using the Boltzmann equation are shown in Fig. 9 (Kuzumoto *et al.* 1989). The excitation efficiency is defined as the fractional power transfer to the total upper laser levels [$CO_2(001)$, $N_2(v{=}1\text{–}8)$ and $CO(v{=}1\text{–}7)$]. As seen in the figure, SD excitation is less efficient in comparison with the conventional DC glow discharge at low N_2 gas concentrations. This seems to be due to the difference in reduced electric field strength. High lasing efficiency is obtained by optimising the laser medium gas to have a very high fraction of N_2. The optimum gas composition is found experimentally to be a mixture of CO_2–CO–N_2–He = 8–4–60–28%.

3. Concluding Remarks

Silent discharges have been developed to maximise the performance of ozonisers and CO_2 lasers. The characteristics and properties of the discharge are discussed and examined in the light of experimental results. A comparison of the two devices is presented in Table 2. We have found a high efficiency of ozone yield by using high energy electrons in a narrow gap. On the other hand, in CO_2 lasers, a high excitation efficiency is achieved by specifying a laser medium gas at very high N_2 concentrations in a wide gap.

References

Eliasson, B., and Kogelschatz, U. (1986). *J. Chem. Phys.* **83**, 279.
Eliasson, B., Hirth, M., and Kogelschatz, U. (1987). *J. Phys.* D **20**, 1421.
Kuzumoto, M., and Yagi, S. (1990). *Trans. IEE Japan* A **1210**, 302.
Kuzumoto, M., Ogawa, S., Yagi, S., and Nagai, H. (1987). *Trans. IEE Japan* **107**, 115.
Kuzumoto, M., Ogawa, S., Tanaka, M., and Yagi, S. (1989). *J. Phys.* D **22**, 1835.
Tabata, N., and Yagi, S. (1975). *Trans. IEE Japan* B **95**, 249.
Tabata, N., Yagi, S., and Tanaka, M. (1978). *Trans. IEE Japan* B **98**, 17.
Tanaka, M., Yagi, S., and Tabata, N. (1984). *Trans. IEE Japan* A **104**, 217.
Yagi, S., Hishii, M., Tabata, N., Nagai, H., and Nagai, A. (1977). *Rev. Laser Engineering* **5**, 171.

Manuscript received 31 August, accepted 28 October 1994